Biochar: A Potential Catalyst Support for Hydrotreatment Catalysts

Yvette Van Tonder, Roelf Venter, and Sanette Marx

***Abstract*—** This article evaluates the effectiveness of biochar as catalyst support for hydrotreatment catalysts. The prepared biochar supported catalysts were tested by catalytically hydrotreating oil extracted from spent coffee grounds (SCG). The biochar supported catalysts were compared with a commercially procured alumina supported catalyst. The catalysts were evaluated based on their triglyceride conversion, diesel yield and liquid product composition. The triglyceride conversion order was Ni-Mo/alumina (98.6%) > Ni-Mo/ CL (97.9%) > Ni-Mo/CS (97.3%). The diesel yield order was Ni-Mo/alumina (846.6 g diesel.kg-1 oil) > Ni-Mo/ CL (686.1 g diesel.kg-1 oil) > Ni-Mo/CS (629.8 g diesel.kg-1 oil). Although the biochar supported catalysts had a slightly lower triglyceride conversion and diesel yield compared to the commercial alumina supported catalyst, the biochar supported catalysts had a higher proportion of iso-paraffins in the liquid product. The results indicate that biochar was a promising support for hydrotreatment catalysts.

***Index Terms*—** Activation, biochar, hydrotreatment catalysts, hydrothermal liquefaction.

I. Introduction

Fossil Fuels such as natural gas, coal and crude oil are non-renewable energy sources, their use is not sustainable and their reserves will be depleted in the future as their demand increase. Global Industry Analysts [1] reported that the global diesel demand will increase from 28.9 million barrels per day in 2016 to 31.3 million barrels in 2020. An increasing growth of civilisation leads to an increasing number of automobiles on the road. This increase in automobiles will result in an increase in petroleum fuel consumption [2]. Petroleum fuel consumption has a large share in the global greenhouse gas (GHG) emissions, contributes to air pollution and negatively effects human health and biodiversity [3].

Fatty-acid methyl esters (FAME) is a petro-diesel alternative intended to lessen the impact of petroleum fuel consumption on the environment. FAME (i.e., biodiesel) contains a higher concentration of oxygenates and has undesirable cold flow properties when compared with petroleum fuels [4]. Renewable fuel exhibits improved properties when compared to FAME and petroleum fuels. Renewable fuel is produced by the catalytic hydrotreatment of triglyceride-based oils.

Yang, Wang [7] defines catalytic hydrotreatment as the deoxygenation of the triglyceride based oil via three different reaction pathways: decarbonylation (HCN), decarboxylation (HCX) and hydrodeoxygenation (HDO) in the presence of a hydrotreating (HT) catalyst. Traditional HT catalysts were designed with high hydrodesulphurization (HDS) and hydrodenitrogenation (HDN) activity as the crude oil used as feedstock to produce petroleum fuels have high concentrations of sulphur (S) and nitrogen (N). However, during the upgrading of triglyceride based oils, the feedstock contains a high concentration of oxygenates and negligible S and N components.

The driving forces for this article include an increasing global energy demand, changing feedstocks, stricter environmental legislation, innovation in the automotive industry and competition between hydrotreatment catalyst manufacturers. These forces motivate and drive the continued research of hydrotreating catalysts. The driving forces for the article indicate that although the research on hydrotreatment catalysts are extensive, it has not yet reached maturity.

In this study two catalysts were produced using biochar as catalyst support obtained from the hydrothermal liquefaction (HTL) of sweet sorghum and sodium lignosulphonate. The catalysts were evaluated and compared with a commercially procured Ni-Mo/alumina catalyst.

II. EXPERIMENTAL

A. Material

Sweet sorghum bagasse, obtained from the agricultural research council (ARC) and sodium lignosulphonate, obtained from Sappi was selected as feedstock material for the production of biochar through hydrothermal liquefaction. A triglyceride based oil extracted from spent coffee grounds through soxhlet extraction was used as feedstock for the batch hydrotreatment experiments. The spent coffee grounds (SCG) oil and catalysts were oven-dried overnight at 90 5°C prior to each hydrotreatment experiment. A commercial Ni-Mo/Al2O3 catalyst was used as reference. The de-ashing agent was a 1 M HCL (aq) solution. The activation agent was a 7 M KOH (aq) solution. The catalyst impregnation solution was prepared with nickel nitrate and ammonium heptamolybdate salts supplied by

Manuscript received November 6, 2017. This work was supported by The National Research Foundation (South Africa).

Yvette van Tonder is with the School for Chemical and Minerals Engineering of the North West University, Potchefstroom, South Africa. (yvettev314@gmail.com)

Roelf Venter is with the School for Chemical and Minerals Engineering of the North West University, Potchefstroom, South Africa. (10303685@nwu.ac.za)

Sanette Marx is with the School for Chemical and Minerals Engineering of the North West University, Potchefstroom, South Africa. (Sanette.Marx@nwu.ac.za).

Sigma-Aldrich. Deionised water was used in all experiments. Tap water was only used during the cleaning of equipment. The reaction gasses were N2, H2 and 15 vol% H2S/Ar supplied by Afrox.

B. Experimental procedure

Biochar was produced by hydrothermal liquefaction of sweet sorghum bagasse and sodium lignosulphonate at 300°C and 10 bar initial nitrogen pressure. The biochar was dried and de-ashed by acid washing with a 1 M HCL (aq) solution prior to being chemically activated by 7 M KOH (aq) impregnation and calcination at 700°C for 2 hours. The activated biochar was impregnated sequentially with ammonium heptamolybdate, followed by nickel nitrate. The Ni-Mo/biochar catalysts were tested by hydrotreating SCG oil to produce renewable diesel. The catalysts were activated prior to hydrotreatment in the batch reactor by sulphidation. The hydrotreatment reactions were carried out at 390°C and 90 bar initial hydrogen pressure.

C. Catalyst characterisation and product analysis

The physical properties of the catalysts and biochar were determined through Brunauer-Emmet-Teller (BET) adsorption analysis; Scanning Electron Microscope (SEM) and Energy Dispersive X-Ray Spectroscopy (EDS) analyses were conducted to investigate catalyst morphological properties and catalyst loading; A proximate analysis was conducted to determine the ash content of the biochar; Gas Chromatography coupled to Mass Spectrometer (GC-MS) and Calorific Value (CV) analyses were conducted to analyse the liquid product obtained from the hydrotreatment of the SCG oil.

III. RESULT AND DISCUSSION

A. Proximate contents

The proximate contents of the biomass and de-ashed biochar are presented in TABLE I. As seen from TABLE I, the ash content of the water washed lignin and sorghum biochar increased after being washed with the acid.

It is assumed that during acid washing of the biochar, the chemical structure of the biochar was altered due to the degradation of the exposed lignin and the chemical structural components forming new bonds with the aqueous acid solution components. These salts precipitate on the surface of the biochar and form part of the ash content during the proximate analysis. These bonds did not form during the water washing of the biochar as the deionised water did not degrade the lignin structure.

The difference in the ash content of the biomass and unwashed biochar samples can be attributed to volatilisation during HTL; the mineral matter in the biomass remaining in the biochar during HTL; new bonds being formed during acid washing; or interactions between the volatiles and the biochar resulting in changes in the ash proportion of the sample [7, 8].

TABLE I
PROXIMATE CONTENTS OF BIOMASS AND BIOCHAR

Sample	Moisture content (wt%)	Volatile matter content (wt%)	Ash content (wt%)
Sweet sorghum bagasse			
Biomass	5.09	78.1	15.3
Unwashed biochar	5.99	45.8	8.38
Water washed biochar	0.4	47.4	7.24
Acid washed biochar	1.59	45.9	12.8
Sodium lignosulphonate			
Biomass	2.55	54.4	57.2
Unwashed biochar	12.1	54.4	8.27
Waster washed biochar	12.5	34.5	5.88
Acid washed biochar	0.89	30.8	22.8

TABLE II
PHYSICAL PROPERTIES OF BIOCHAR AND CATALYST SAMPLES

Property	De-ashed - L	Activated - L	Cat. loaded - L	De-ashed - S	Activated - S	Cat. loaded - S
CO_2 adsorption						
D-R micropore surface area ($m^2.g$-1)	138	835	63	79.1	1012	361
BET surface area ($m^2.g$-1)	87.8	720	44.5	57.4	631	232
Pore volume x10^{-2} ($cm^3.g^{-1}$)	3.09	20.7	1.59	1.84	23	8.44
Pore diameter (Å)	3.87	4.10	3.93	4.03	3.7	3.76
Microporosity (%)	5.11	28	2.56	2.71	42.4	15
N_2 adsorption						
BET surface area ($m^2.g^{-1}$)	1.44	946	56	4.22	727	269
BJH pore volume x10^{-2} ($cm^3.g^{-1}$)	0.717	15.3	7.42	2.69	8.09	7.97
BJH pore diameter (Å)	316	42.8	73.1	325	40.9	53.2
Mesoporosity (%)	0.89	44.5	18.1	3.32	21.4	20.6

B. Physical properties - BET

Significant porosity development is observed for the activated samples in TABLE II. The increasing pore volume of all de-ashed biochar samples after activation indicates that material that might have been present in the pores, lowering the volume have been removed [16].The BET surface area of de-ashed biochar is generally lower than that of activated biochar [17, 18], and this is also exhibited by the results in TABLE II. Chemical activation is conducted to develop this porosity of de-ashed biochar [19]. To produce carbonaceous biochar, the mineral content of the biochar has to be sufficiently low. Any remaining ash components after acid washing of the

biochar will cause a blockage of the pores during activation, resulting in a decreased surface area [7, 20]. The chemical activation of the biochar was successful despite the increase in ash content after acid washing presented in TABLE I.

During activation of the biochar, the activated carbon yield was extremely low. This is also reported in literature [10]. As the activation was performed at 700°C, all moisture and volatile matter were eliminated from the biochar. This resulted in excessive mass loss and subsequent porosity development. It has been reported that a high volatile matter and fixed carbon content is beneficial for the preparation of highly porous biochar [7, 11].

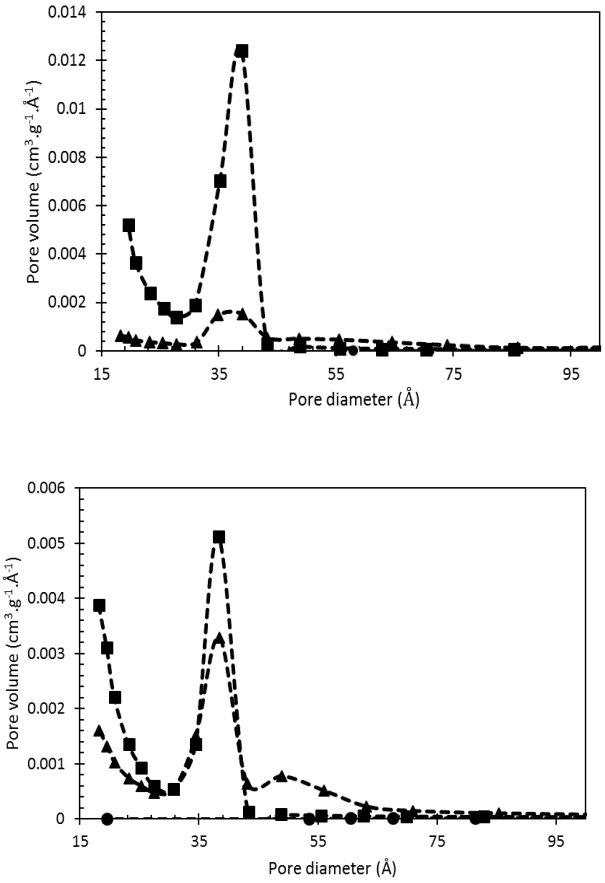

Fig. 1. Porosity development of lignin (A) and sorghum (B) derivatives. (■) Activated biochar, (▲) catalysts, (●) De-ashed biochar.

The development of porosity during activation is attributed to the release of volatile matter, which interconnects pores within the biochar facilitating the diffusion of KOH into the structure [9, 12, 13]. During the elimination of the volatile matter, the exiting material created cavities (i.e., developed pores) representing the exit path and solid rearrangement [14]. The volatilisation during activation resulted in well-developed porous biochar. The CO_2 adsorption surface area determined by the Dubinin-Radushkevich (D-R) method was significant. This indicates that the microporosity increased in the activated biochar samples after activation.

Activation of biochar is important as it generates a larger surface area for the dispersion of the impregnated metal precursors [13]. The higher the surface area of the catalyst is, the more interactions or chemical reactions can occur per gram of the catalyst [21].

The impregnation of the metals may cause limited accessibility of the reactants to the micropores, resulting in a less active catalyst [22]. Generally, with the impregnation of the active metal precursors, a decrease in specific surface area and specific pore volume results [23-25]. This was observed with the surface area results of the catalysts presented in TABLE II.

The porosity of the prepared Ni-Mo/Cx catalysts are lower than the activated biochar samples. This can presumably be due to the blockage of the support micropores by the active metal precursors. The D-R surface area of the catalysts reduced significantly indicating that the micropores have been filled/blocked by the active metal precursors. Micropores and mesopores are present in the activated biochar and catalysts. This coexistence (bi-modal) of pores is good for hydrotreating catalysts as it eliminates diffusion limitations caused by microporous structures [13, 26]. The mesoporosity of the activated biochar will facilitate reactant diffusion to the active sites located internally while not being limited to low molecular weight compounds [27].

It can be seen from Fig. 1 that there is a significant increase in meso-, and micropores after activation. This is observed due to the de-ashed line being flattened out. It was seen from the N_2 adsorption results presented in TABLE II that the de-ashed biochar samples were predominantly mesoporous but with very low porosity. Thus, the meso-, and microporosity of both activated biochars were significantly developed with the activation procedure. However, a reduction in micro-, and mesopore volume is observed in Fig. 1 after metal precursor impregnation. This is presumably due to the precipitation of the active precursors in these pores. The reduction in micropore volume is higher than the reduction in mesopore volume indicating that the metal precursors predominantly precipitated in the micropores of the activated biochar for both the lignin and sorghum supported catalysts. This indicated that for the catalysts, the active sites (i.e., metal phases) are located in the micropores and the mesopores are primarily for the diffusion of the reactants and products to and from the active sites.

C. Catalysts loading - EDS

The metal components on the catalyst samples were quantified by an EDS analysis. The weight percentages of the molybdenum and nickel metals on the catalysts are presented in TABLE III.

From TABLE III, it is seen that the metal loading of the sorghum supported catalyst is close to the concentration of the impregnation solution (i.e., 15 wt% Mo and 5 wt% Ni). This was not the case for the lignin supported catalyst. This is presumably due to the initially higher surface area of the activated lignin biochar which resulted in a higher concentration of metals precipitating on the surface of the biochar. When the metal loading is low, the porosity of the catalyst is known to act

as the physical barrier for dispersion and resistance to sintering [22]. If the loading of the catalysts were to be increased, the dispersion of the metals would decrease due to the part of the

TABLE III
CATALYST LOADING

Metal loading	Ni-Mo/C_S	Ni-Mo/C_L
Mo (wt%)	16.2	22.9
Ni (wt%)	5.2	22.8

D. Morphological properties - SEM

Another method to characterise the surface area and porosity of the biochar and catalyst samples is SEM analysis. Fig. 2 presents the SEM images of the biochar and catalyst samples.

From Fig.2-A.1, the presence of spheres is an indication of condensed lignin on the surface of the biochar due to the delignification of the biochar during the acid wash treatment. From Fig. 2-B.1, the high ash and volatile content of the acid washed biochar presented in TABLE I is validated by the presence of the clotted structures and crystallised salts on the surface of the biochar indicating volatile matter and ash, respectively. When comparing Fig. 2-A.1 with Fig. 2-B.1, it can be seen that the surface area of the lignin biochar (A.1) is more exposed due to the higher degree of delignification obtained by the lignin biochar during acid washing. The de-ashed lignin biochar is also more porous than the de-ashed sorghum biochar, validating the higher surface areas obtained for the de-ashed lignin biochar than for the sorghum biochar with the BET analysis presented in TABLE II.

The development of the porosity of the de-ashed biochars after activation can be observed from the SEM analysis presented in Fig. 2. Porosity is developed in the deashed biochar as indicated by the presence of the sponge-like structures in Fig. 2-A.2 and Fig. 2-B.2, which was not part of the original biochar structure. When comparing the activated lignin and sorghum biochar, the porosity development is more pronounced for the lignin biochar than for the sorghum biochar. This is validated by the difference in surface areas between the activated biochar samples obtained from the BET analysis presented in TABLE II. The clotted structures representing volatiles on the de-ashed sorghum biochar (B.1) is absent on the surface of the activated sorghum biochar (B.2). This signifies that volatilisation occurred during activation, increasing the surface area of the biochar. This is validated by the increase in activated sorghum biochar surface area presented in TABLE II. Seen from Fig. 2-B.2, the development of the surface area is observed due to the delignification of the biochar. As the lignin is removed, a more porous structure remains. The KOH solution also removed most of the ash crystals present on the surface of the biochar. In Fig .2-A.2 and Fig. 2-B.2 an incomplete activation process is observed. Only partial activation was achieved during the activation process which is observed from the presence of structures that don't exhibit a sponge-like (porous) appearance.

Seen from Fig. 2-A.3 and Fig. 2-B.3 the impregnated metals formed crystallised structures and precipitated on the surface of the activated biochar, resulting in a decrease in surface area.

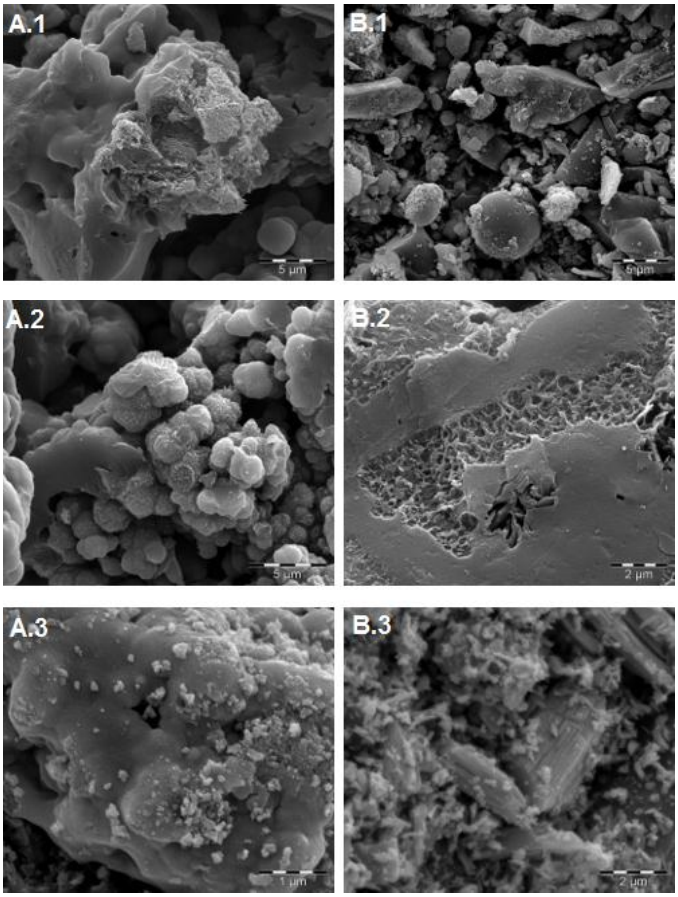

Fig. 2. SEM Images of lignin (A) and sorghum (B) de-ashed biochar (.1), activated biochar (.2), and catalyst (.3) samples.

TABLE IV
TRIGLYCERIDE CONVERSION

Catalyst	Conversion (%)
Ni-Mo/CS	97.3
Ni-Mo/CL	97.9 ± 2
Ni-Mo/alumina	98.6

The surface areas of the catalyst samples presented in TABLE II are lower than the activated biochar samples. This is also observed from Fig. 2-A.3 and Fig. 2-B.3 where the porous structures (i.e., sponge-like structures) have decreased due to the assumed deposition of the active metals within this porous structures. The concentration of the impregnation solution was presumably too high indicated by the high precipitate loading of the metal salts on the surface of the activated biochar. The assumption of a too high metal loading is validated by the significant decrease in catalyst surface area after impregnation presented in TABLE II.

E. Product analysis- GC-MS

TABLE IV presents the triglyceride conversion obtained with the hydrotreating catalysts.

Seen from TABLE IV, the triglyceride conversion order is Ni-Mo/alumina > Ni-Mo/ C_L > Ni-Mo/C_S. The difference between the catalyst conversions are small. This indicates that the conversion obtained with the biochar supported catalysts are in agreement with the conversion obtained with the alumina supported catalyst. The high conversions obtained by all three

catalysts indicate that the catalysts have a high deoxygenation activity. Ultimately, the results indicate that the alumina catalyst has the highest triglyceride conversion. This is presumably due to the turnover frequency (TOF) of the catalysts. The alumina supported catalyst potentially has a higher amount of active sites than the biochar supported catalysts, resulting in a higher conversion. The experimental error determined for the hydrotreatment conversion with the lignin supported catalyst was low, i.e., 4.13%. The error was determined for a 95% confidence interval. Thus, any additional hydrotreatment experiment with the lignin supported catalyst will yield a conversion that will fall within the range 95.9 - 99.9%, 95% of the time.

Seen from Fig. 3, the order of diesel yield is: Ni-Mo/alumina > Ni-Mo/C_L > Ni-Mo/C_S. Although the alumina catalyst had the highest yield, the diesel yield produced with the biochar supported catalysts are in agreement with that of the alumina supported catalyst. The diesel produced by hydrotreatment of the SCG oil with the commercial hydrotreating catalyst was highest. The main component of the liquid product obtained with all three catalysts were diesel. The order of the naphtha composition of the liquid product was Ni-Mo/C_L (0.53 wt%) > Ni-Mo/alumina (0.31 wt%) > Ni-Mo/C_S (0.21 wt%). The higher naphtha composition of the fuel produced with the Ni-Mo/C_L could be due to cracking being enhanced by the Ni-Mo/C_L catalyst compared to the Ni-Mo/alumina and Ni-Mo/C_S catalysts [6]. The lower diesel yield obtained with the biochar supported catalysts are presumably due to the enhancement of side reactions which lower the diesel yield. The enhanced cracking tendency of the Ni-Mo/C_L catalyst could be due to the stronger acid sites promoting the side reactions [29].

Seen from Fig. 4, the most abundant component in the liquid product for all three catalysts is n-paraffins. Although the conversion obtained by all three catalysts were similar, the liquid product composition is different. Thus, the difference between the catalysts were their ability to suppress side reactions such as cracking and enhance isomerisation reactions to improve the cold flow properties of the renewable diesel. The presence of n-C_{16} and n-C_{18} alkanes relative to n-C_{15} and n-C_{17} alkanes indicate that HDO did occur, however the n-C_{17}/n-C_{18} ratio indicates that the dominant reaction pathway was HCX and or HCN. There was a small amount of shorter n-alkanes that formed presumably due to the hydrocracking of longer chain n-alkanes [6]. The order of amount of unconverted oxygenates in the liquid product is Ni-Mo/C_S > Ni-Mo/C_L > Ni-Mo/alumina. This is in agreement with the triglyceride conversion order presented in TABLE IV, where the product obtained with the Ni-Mo/C_S catalyst had the lowest conversion.

The higher amount of olefins is due to the inability of the Ni-Mo/C_L catalyst to saturate the olefins formed during hydrocracking reactions [29].

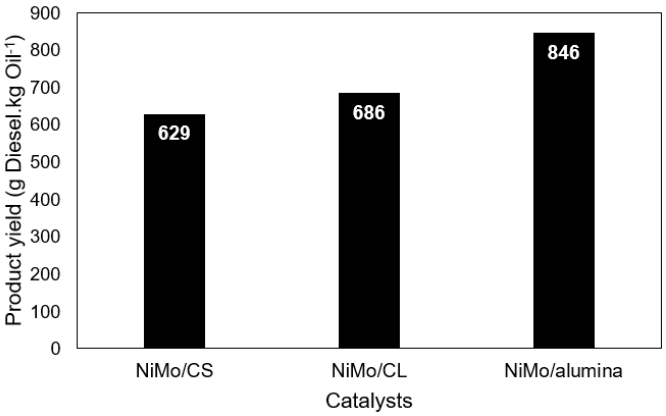

Fig. 3. Hydrotreatment liquid product diesel yield.

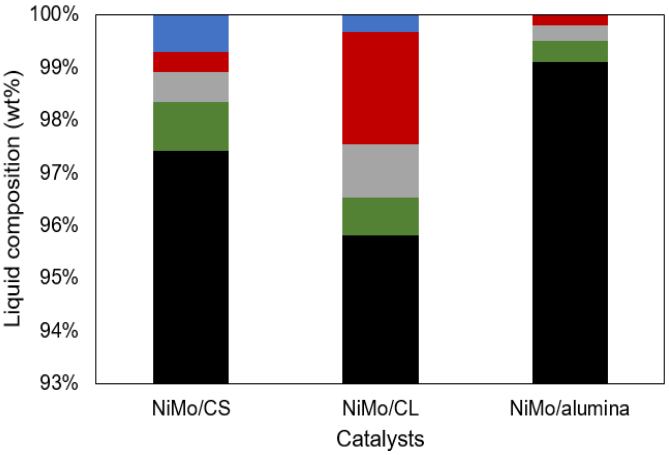

Fig. 4. Liquid fuel product composition. (■) n-paraffins, (■) iso-paraffins, (■) cyclo-paraffins, (■) olefins and (■) Oxygenates.

The higher amount of olefins could also be due to the dehydrogenation of the hydrocarbons occurring after deoxygenation [30]. The low amount of olefins in the liquid product obtained with the Ni-Mo/C_S and Ni-Mo/alumina liquid products suggest that dehydrogenation was negligible during these reactions. Aromatics was not present in any liquid product by any of the three catalysts. The order of iso-paraffins is Ni-Mo/C_S > Ni-Mo/C_L > Ni-Mo/alumina. This indicated that the biochar supported catalysts were more active in enhancing isomerisation and converting the n-alkanes to iso-paraffins. This promoting of side reactions can be an indication that the biochar supported catalysts have stronger acid sites [29]. The moderate acidity of the alumina catalyst isn't sufficient for the promotion of isomerisation at the operating conditions of the experiment, indicating that to have obtained more iso-paraffins, the reaction conditions (i.e., temperature and pressure) had to be increased.

The Ni-Mo/C_L catalyst promoted hydrocracking which lowered the diesel yield [29]. This indicates that although the alumina supported catalyst had a slightly higher diesel yield, the diesel produced with the biochar supported catalyst had improved cold flow properties compared to the diesel produced with the Ni-Mo/alumina catalyst.

F. CV

Oil cannot be used as petro-diesel substitute due to its high viscosity, instability, polarity and immiscibility with hydrocarbons [27]. The instability of oil is allied to the deteriorating higher heating values (HHV) due to

polymerisation and condensation of the oxygenated compounds [27]. TABLE V presents the HHV's of the renewable diesel and SCG oil. SCG oil has a higher HHV than raw biomass but lower than crude oil [27]. The oil should therefore be upgraded to remove the oxygenated compounds. The presence of chemically bound high molecular-weight oxygenates in the SCG oil is allied to the low HHV [27, 32]. As can be seen from TABLE V, SCG oil was a good choice for feedstock as its HHV was already 85% of that of petro-diesel.

Seen from TABLE V, the order of the HHV is Ni-Mo/alumina > Ni-Mo/C_L > Ni-Mo/C_S > SCG oil. The HHV of the diesel produced with the three different catalysts are very similar. Both prepared catalysts performed HDO, HCX and HCN reactions as the HHV of the SCG oil was sufficiently improved to values comparable with that of petro-diesel. The renewable diesel produced by catalytic hydrotreatment with the Ni-Mo/Al_2O_3 catalyst had the highest HHV. The HHV is an indication of the degree of deoxygenation of the SCG oil during hydrotreatment. Additionally, it is a measure of the energy content of the diesel fuel [33]. It is therefore observed that the Ni-Mo/Al_2O_3 catalyst eliminated the most oxygenated compounds from the oil. Between the sorghum supported and lignin supported catalysts, the Ni-Mo/C_L catalyst produced a diesel with the highest HHV. This is in agreement with the conversion and amount of oxygenates in the liquid product, presented in TABLE IV and Fig. 4, respectively. The alumina supported catalyst obtained the highest conversion with no oxygenates in the liquid product, and the sorghum supported catalyst obtained the lowest conversion with the highest amount of oxygenates in the liquid product. The HHV of the renewable diesel produced with the biochar supported catalysts is in the range of 44-45 MJ/kg and compared to the HHV of petro-diesel, i.e., 45 MJ/kg [32] it is in agreement with the energy requirement for diesel fuel. The analytical error determined for the HHV of the fuel produced with the sorghum supported catalyst was low, i.e., 1.12%. The error was determined for a 95% confidence interval. Thus, any additional CV analysis of the fuel produced with the sorghum supported catalyst will fall within the range 43.9-44.3 MJ/kg, 95% of the time.

TABLE V
CALORIFIC VALUE OF DIESEL FUEL PRODUCED WITH BIOCHAR AND ALUMINA SUPPORTED CATALYSTS.

Sample	Calorific value ($MJ.kg^{-1}$)
SCG oil (n-Hexane)	38.6
SCG oil (Methanol)	37.3
Ni-Mo/C_S	44.1 ± 0.2
Ni-Mo/C_L	44.9
Ni-Mo/alumina	46.1

IV. CONCLUSION

Although the ash content of the biochar was higher after acid washing, significant activation of the biochar was achieved regardless. As presented in TABLE II, the CO2 adsorption BET surface area of the deashed lignin (87.8 m2.g-1) and sorghum (57.4 m2.g-1) increased significantly to 720 m2.g-1 for the activated lignin biochar and 631 m2.g-1 for the activated sorghum biochar. The N2 adsorption porosity and surface area values of the de-ashed to activated biochar also significantly increased. The final metal loading obtained on the catalysts were 16.2 wt% (sorghum) and 22.9 wt% (lignin) molybdenum and 5.2 wt% (sorghum) and 22.8 wt% (lignin) nickel. The sorghum biochar supported catalyst had a loading similar to the concentration of the impregnation solution. However, the lignin biochar supported catalyst' loading was excessive and higher than intended. Presented in TABLE II, the final surface areas of the catalysts had reduced significantly. This is presumably due to the high loading of the metal precursors on the surface of the activated biochar. The catalysts were evaluated based on their triglyceride conversion, diesel yield and liquid product composition. The triglyceride conversion order was Ni-Mo/alumina > Ni-Mo/ CL > Ni-Mo/CS. This is in agreement with the oxygenate proportion of the liquid products presented in Fig. 4, where the product obtained with the Ni-Mo/CS catalyst had the highest proportion of oxygenates. The diesel yield order was Ni-Mo/alumina > Ni-Mo/ CL > Ni-Mo/CS.

Although the Ni-Mo/CS and Ni-Mo/CL had a slightly lower triglyceride conversion and diesel yield compared to the commercial catalyst, biochar supported catalysts had a higher proportion of iso-paraffins in the liquid product. Indicating that the diesel produced with the biochar supported catalysts potentially had improved cold flow properties compared to diesel produced with the commercial alumina supported catalyst. The high conversion, promotion of isomerisation and low cost of Ni-Mo/biochar catalysts indicate that biochar is a promising support for hydrotreatment catalysts.

ACKNOWLEDGMENT

The financial assistance of the National Research Foundation (NRF) towards this research is hereby acknowledged. Opinions expressed and conclusions arrived at are those of the author and are not necessarily to be attributed to the NRF.

REFERENCES

[1] Global Industry Analysts, I. Petroleum Refining Catalysts - A Global Strategic Business Report. 2015 [cited 2017; Available from: http://www.strategyr.com/MarketResearch/Petroleum_Refining_Catalysts_Market_Trends.asp.

[2] Pattanaik, B.P. and R.D. Misra, Effect of reaction pathway and operating parameters on the deoxygenation of vegetable oils to produce diesel range hydrocarbon fuels: A review Renewable and Sustainable Energy Reviews, 2017. 73: p. 545-557.

[3] Springer, N. and R. Schuchard. Why Petroleum? 2015 [cited 2017 25 April]; Available from: https://www.bsr.org/en/our-insights/report-view/fuel-sustainability-brief-petroleum.

[4] Ayetor, G.K., A. Sunnu, and J. Parbey, Effect of biodiesel production parameters on viscosity and yield of methyl esters: Jatropha curcas, Elaeis guineensis and Cocos nucifera. Alexandria Engineering Journal, 2015. 54: p. 1285-1290.

[5] Ottinger, R.L., Biofuels – Potential, Problems & Solutions in Biofuels Conference. 2007.

[6] Veriansyah, B., et al., Production of renewable diesel by hydroprocessing of soybean oil: Effect of catalysts. Fuel, 2012. 94: p. 578-585.
[7] Lori, J.A., A.O. Lawal, and E.J. Ekanem, Proximate and Ultimate Analyses of Bagasse, Sorghum and Millet Straws as Precursors for Active Carbons. Applied Sciences, 2007. 7(21): p. 3249-3255.
[8] Qian, K., et al., Effects of Biomass Feedstocks and Gasification Conditions on the Physiochemical Properties of Char. Energies, 2013. 6: p. 3972-3986.
[9] Schimmelpfennig, S. and B. Glaser, One Step Forward toward Characterization: Some Important Material Properties to Distinguish Biochars. Journal of Environmental Quality, 2012. 41: p. 1001-1013.
[10] Hui, T.S. and M.A.A. Zaini, Potassium hydroxide activation of activated carbon: a commentary. Carbon Letters, 2015. 16(4): p. 275-280.
[11] Zhang, X., et al., Effects of hydrofluoric acid pre-deashing of rice husk on physicochemical properties and CO2 adsorption performance of nitrogen-enriched biochar. Energy, 2015. 91: p. 903-910.
[12] Mao, H., et al., Preparation of Pinewood- and Wheat Straw-based Activated Carbon via a Microwave-assisted Potassium Hydroxide Treatment and an Analysis of the effects of the Microwave Activation Conitions. BioResources, 2015. 10(1): p. 809-821.
[13] Zhu, L., et al., Biochar: a new promising catalyst support using methanation as a probe reaction. Energy Science and Engineering, 2015. 3(2): p. 126-134.
[14] Leofanti, G., et al., Catalyst characterization: characterization techniques. Catalysis Today, 1997. 34: p. 307-327.
[15] Uemura, Y., et al. CHEMICAL ACTIVATION OF BIOCHAR MADE FROM OIL PALM KERNEL SHELL AND ITS APPLICATION TO ADSORBENT FOR P-NITROPHENOL. 2013.
[16] Kaushik, A., et al., Activated carbon from sugarcane bagasse ash for melanoidins recovery. Journal of Environmental Management, 2017. 200: p. 29-34.
[17] Lee, J., K.-H. Kim, and E.E. Kwon, Biochar as a Catalyst. Renewable and Sustainable Energy Reviews, 2017. 77: p. 70-79.
[18] Inyang, M., et al., Enhanced Lead Sorption by Biochar Derived from Anaerobically Digested Sugarcane Bagasse. Separation Science and Technology, 2011. 46(1950-1956).
[19] Dehkhoda, A.M., Developing Biochar-Based Catalyst for Biodiesel Production 2010, THE UNIVERSITY OF BRITISH COLUMBIA (Vancouver).
[20] Tan, X.-f., et al., Biochar as potential sustainable precursors for activated carbon production: Multiple applications in environmental protection and energy storage. Biosource Technoogy, 2017. 227: p. 359-372.
[21] Brewer, C.E., Biochar characterization and engineering 2012, Iowa State University.
[22] Rodriguez-Reinoso, F., THE ROLE OF CARBON MATERIALS IN HETEROGENEOUS CATALYSIS. Carbon, 1998. 36(3): p. 159-175.
[23] Vasilevich, A.V., et al., Effect of the Textural Parameters of the Carrier and the Preparation Procedure of the Supported Ni–Mo/Sibunit Catalysts on Their Catalytic Activity Solid Fuel Chemistry, 2015. 49(1): p. 49-53.
[24] Rajapaksha, A.U., et al., Engineered/designer biochar for contaminant removal/immobilization from soil and water: Potential and implication of biocar modification. Chemosphere, 2016. 148: p. 276-291.
[25] Petkovic, L.M. and D.M. Ginosar, Comparison of Two Preparation Methods on Catalytic Activity and Selectivity of Ru-Mo/HZSM5 for Methane Dehydroaromatization. Fuels, 2014. 2014.
[26] Gonzalez, M.E., et al., Functionalization of biochar derived from lignicellulosic biomass using microwave technology for catalytic application in biodiesel production. Energy Conversion and Management, 2017. 137: p. 165-173.
[27] Patel, M. and A. Kumar, Production of renewable diesel through the hydroprocessing of lignocellulosic biomass-derived bio-oil: A review. Renewable and Sustainable Energy Reviews, 2016. 58: p. 1293-1307.
[28] Kalinke, C., et al., Activated biochar: Preparation, characterisation and electroanalytical application in an alternative strategy of nickel determination. Analytica Chimica Acta, 2017. xxx: p. 1-9.
[29] Sotelo-Boyas, R., Y. Liu, and T. Minowa, Renewable Diesel Production from the Hydrotreating of Rapeseed Oil with Pt/Zeolite and NiMo/Al2O3 Catalysts. Industrial and Engineering Chemistry Research, 2011. 50: p. 2791-2799.
[30] Kim, S.K., et al., Production of renewable diesel via catalytic deoxygenation of natural triglycerides: comprehensive understanding of reaction intermediates and hydrocarbons. Applied Energy, 2014. 116: p. 199-205.
[31] Gandarias, I., et al., From biomass to fuels: Hydrotreating of oxygenated compounds. International Journal of Hydrogen Energy, 2008. 33: p. 3485-3488.
[32] Murugesan, A., et al., Bio-diesel as an alternative fuel for diesel engines-A review. Renewable and Sustainable Energy Reviews, 2007. 13: p. 653-662.
[33] K.SIVARAMAKRISHNAN and P.RAVIKUMAR, DETERMINATION OF HIGHER HEATING VALUE OF BIODIESELS. International Journal of Engineering Science and Technology (IJEST), 2011. 3(11).

Yvette van Tonder became a Member (M) of IAE. Born in South-Africa. Studied B. Eng chemical engineering at the North-West University, Potchefstroom Campus, South-Africa.